2008 IEEE International Conference on
Robotics and Automation
Pasadena, CA, USA, May 19-23, 2008

Scan-to-Map Matching Using the Hausdorff Distance for Robust Mobile Robot Localization

M. Torres-Torriti and A. Guesalaga

Abstract— **This paper presents a robust method for localization of mobile robots in environments that may be cluttered and that not necessarily have a polygonal structure. The estimation of the position and orientation of the robot relies on the minimization of the modified Hausdorff distance between ladar range measurements and a map of the environment. The approach is employed in combination with an extended Kalman filter to obtain accurate estimates of the robot's position, heading and velocity. Good estimates of these variables were obtained during tests performed using a differential drive robot in a populated environment, thus demonstrating that the approach provides a reliable and computationally feasible alternative for mobile robot localization and autonomous navigation.*** ***Index Terms - Mobile robot localization, Hausdorff distance, map-matching, scan-matching.***

I. INTRODUCTION

Fully autonomous mobile robots rely significantly on self-localization techniques to accomplish navigation tasks [1]. It is well known that methods based on proprioceptive sensors alone, such as encoders or inertial measurement units, cannot robustly solve the localization problem [2]. This is because errors from odometry readings accumulate leading to unbounded position errors. In view of this limitation, several alternatives to dead reckoning techniques have been developed employing exteroceptive sensors, such as sonar [3], ladar [4], visual sensors [5], or their combination through sensor fusion techniques [6]. Most of these techniques formulate the localization problem in a Bayesian framework as that of finding the robot's most probable location and heading given the current sensor measurements and predicted state using single hypothesis methods (e.g. Extended Kalman Filters, Unscented Kalman Filters) or multi-hypotheses approaches (e.g. Markov Localization, Monte Carlo Localization); see [1] for an excellent review. However, regardless of the particular Bayesian formulation, all techniques involve a process commonly known as *scan matching* or *model matching* in order to find the displacement of the robot with respect to a previous position. The scan matching process consists in finding correspondences between features extracted from current sensor measurements and features extracted from previous scans or features in some pre-built global map of the environment. The matching can be performed either in a feature-to-feature or point-to-point fashion.

The most popular feature-to-feature techniques carry out line-to-line matchings [7], [8]; for a detailed comparison see [9]. The advantage of line-to-line matching lies in its speed, however a major drawback is its limited ability to cope with unstructured or cluttered environments. On the other hand, point-to-point matching does not suffer from this disadvantage, but as noted in [5], in general it is less reliable due to the difficulties arising in (i) associating detected points with previously detected points, and (ii) extracting edge and corner features in cluttered and populated environments. These problems are further complicated by the fact that the total number of points in a map is large, thus rendering the approach computationally expensive. Arguably the most popular point-to-point matching strategy is the Iterative Closest Point (ICP) algorithm [10]. The ICP relies on the Euclidean distance to establish point correspondences and thus cannot address the fact that points far from the sensor may be far from their correspondents due to angular rotation of the sensor. To alleviate this problem, different authors have proposed metrics that capture not only sensor translation, but also rotation [10], [11]. These approaches, however, do not address directly the problem of robustness in the presence of clutter or dynamic elements populating the environment.

To effectively cope with cluttered and unstructured environments, this paper presents a novel approach for localization and pose estimation based on matching *raw* ladar range scans to a relatively simple map or floor plan of the environment that has been previously generated. Our approach differs from existing methods in that it relies on the computation of a set of transformations (translation, rotation and scaling) that minimize the modified Hausdorff distance (HD) between the observations and the model as proposed in [12] for image alignment and shape recognition. The localization procedure also draws on ideas from our earlier work on radar-based ship positioning [13]. Since measurements yield robust and accurate position and heading information, the precision of estimates is further improved employing an extended Kalman filter. Despite relying on a single hypothesis, the proposed approach can recover fairly well from "kidnapping" situations in which the robot is lifted up and moved without being informed. This is because when an ambigous matching occurs, the robot is allowed to move and explore until a unique solution to the matching is found. The inclusion of this approach as part of Markov and Monte Carlo Localization schemes may yield further localization improvements; this is currently being investigated by the authors.

The contribution of our approach is in that it does not require of a complex perception process to extract features of the environment, such as different forms of line detection and association procedures predominant in vision-based approaches. The proposed approach also does not require to find point-to-point correspondences explicitly, which are harder to establish in the presence of dynamic changes and disturbances of the environment [9]. Furthermore, the experimental results obtained using a differential-drive robot demonstrate that the method can be implemented to perform

This work was supported by Conycit of Chile under Fondecyt Grant 11060251.

The authors are with Dept. of Electrical Engineering, Pontificia Universidad Católica de Chile , Vicuña Mackenna 4860, Casilla 306-22, Santiago, Chile {mtorrest, aguesala}@ing.puc.cl

in real-time, and that it is robust to sensor noise, to objects not included in the map and to dynamic environment perturbations, such as people crossing the sensor's field of view or arbitrary position changes of small furniture like chairs, tables or cabinets.

The paper is organized as follows. Section 2 presents the matching strategy based on the modified Hausdorff distance and discusses its robustness. For the readers convenience, an appendix has been included which briefly explains the well-known concept of Hausdorff distance and its application to contour matching. Section 3 presents the sensor model and explains the solution of the localization problem. Experimental results confirming the good performance of the proposed approach are presented in section 4. Finally, section 5 presents the conclusions of our work and discusses some aspects concerning ongoing research.

II. The Matching Strategy and its Robustness

In order to determine the best matching solution, a sequence of translation, rotation and scaling transformations is applied to each set B of range measurements, in such a way as to minimize the *modified Hausdorff distance* (MHD) between the set and a reference set A that contains the contour lines of the environment. The MHD between the measurements set B and the reference set A, denoted by $\bar{h}_K(T(B), A)$, is a well-known measure of dissimilarity between two sets of points. Its formal definition is presented in equation (8) of the appendix, which has been included for the reader's convenience. The transformations that minimize the dissimilarity between the sets readily yield global position and heading information relative to the reference set (global map). Formally, the matching problem is stated as that of finding a transformation $T : \Omega \rightarrow T(\Omega)$ such that it minimizes:

$$\min_T \bar{h}_K(T(B), A) \tag{1}$$

Here T is chosen to be $T_{d,\theta,\alpha} : \Omega \rightarrow \alpha R_\theta(\Omega + d)$, i.e. a translation d in the plane, followed by a rotation by an angle θ and finally a scaling transformation of magnitude α. In order to solve (1), a reliable and rapidly converging approach to minimize (8) was implemented in terms of standard gradient methods.

The robustness and accuracy of the matching method based on the MHD minimization was tested using simulated data. The simulations consider a 500×500 pixels reference image containing a contour formed by two circular arcs of 60 pixels radius; see figure 1. The simulated data, which represents a contour obtained by a ladar, is generated by adding noise to a given percentage of samples of the original reference contour, then rotating this simulated measurements 10° counter-clockwise, and finally, translating the set of points 100 pixels to the right and 150 pixels down. Two different parameters are adjusted for the different scenarios of measured data: the percentage of outliers or measurements affected by noise and the average magnitude of the noise. The noise affecting each measurement sample, if any, is assumed to be zero-mean Gaussian with standard deviation equal to the scenario's noise level.

The results obtained in the simulations are summarized in Table 1. The robustness of matching method based on the MHD is apparent from these results, which show little variation in the position or heading error for different percentage values of noisy samples and noise levels. Even if simulated clutter was intentionally added in the form of uniformly distributed range measurements noise, the quality of the match is preserved as can be appreciated from figure 1, which shows the initial unmatched scan and its final alignment with respect to the reference contour once the matching is completed. Figure 2 shows the convergence of the MHD to a minimum in an almost linear fashion for the different scenarios. The final value of the MHD increases proportionally to the noise level. However, it is worth noting that the final value remains zero for the simulations in which only 20% of the samples are corrupted by noise. This is because the ratio λ for calculation of the MHD was set at 0.7. The ratio λ is a parameter of the MHD (see appendix). A value of $\lambda = 0.7$ means that only 70% of the total number of samples that best match the reference set are used, while the remaining 30% samples that include those corrupted by noise are automatically discarded from the calculation of the MHD. Figure 3 clearly shows that the regular HD curves have largest values beyond the threshold. While scenarios with noise percentages below 30% yield final $\bar{h}_K(A, B)$ equal to zero, scenarios with noise percentages above 30% yield final $\bar{h}_K(A, B)$ which are non-zero and are proportional to the standard deviation of the noise for a fixed threshold λ; see Table 1. The results in Table 1 also confirm that the accuracy is high, as expected according to the theoretical result in [14], which states that the matching error due to spatial sampling is at most one rasterization unit (see Claim 3 in [14]) for the noise-free situation. This result may also be e

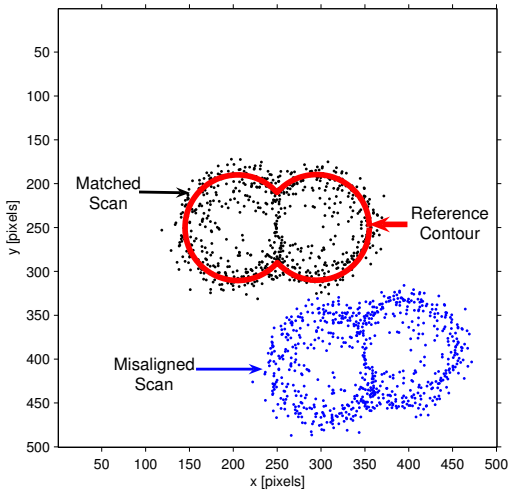

Fig. 1. Initial misalignment and final match between simulated scan (dots) and the reference contour (line).

III. Localization Problem

For convenience of exposition, let x and y denote the position coordinates of the robot in the global 2D Cartesian frame of reference, and let θ denote its orientation with respect to the vertical axis. The first step to determine the robot's position and heading is to express each of the N raw range measurements $z_i^s = [r_i, \theta_i^s]$, $i = 1, 2, \ldots, N$, obtained in polar coordinates relative to the sensor coordinate frame O_s, as *Cartesian coordinates relative to the global coordinate frame* O_w. To this end, the following measurement model is employed:

$$z_i^w = \begin{bmatrix} (r_i^s + \beta_r)\cos(\theta_i^s + \theta + \beta_\theta) + x + \eta_x \\ (r_i^s + \beta_r)\sin(\theta_i^s + \theta + \beta_\theta) + y + \eta_y \end{bmatrix} \tag{2}$$

TABLE I

SIMULATION RESULTS OF THE POSITIONING ACCURACY.

Noise Percentage [%]	Noise Level σ [pixels]	Final Match Position Error [pixels]	Final Match Heading Error [○]	Initial $\bar{h}_K(A,B)$ [pixels]	Final $\bar{h}_K(A,B)$ [pixels]
0	0	2	2.67	88.99	0.65
20	10	0	0.33	88.66	0
20	20	0	0.33	88.98	0
50	10	0	0.33	88.76	0.76
50	20	0	0.17	87.73	1.64
100	10	2.83	0.67	88.93	4.65
100	20	1.41	1.33	87.65	8.36

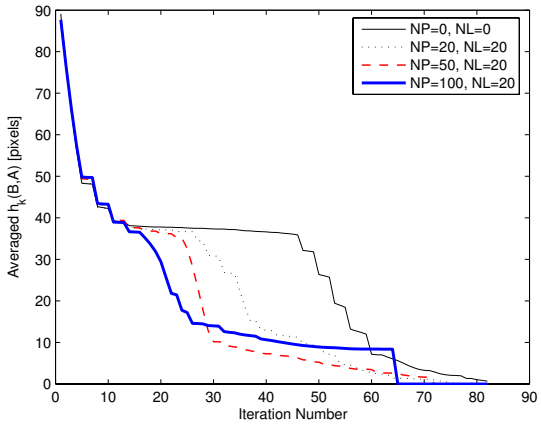

Fig. 2. Convergence of the modified Hausdorff distance $\bar{h}_K(B,A)$ setting $\lambda = 0.7$ for the different scenarios with percentages of noisy samples NP and noise levels NL.

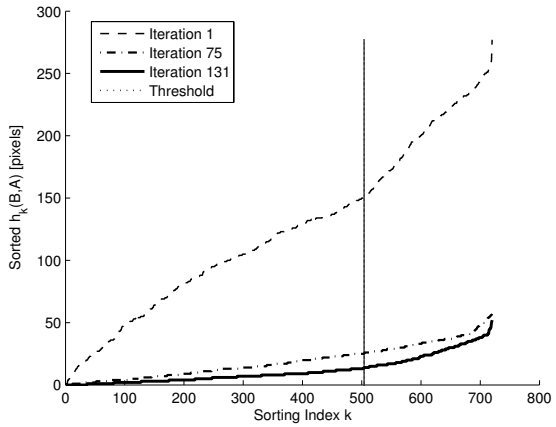

Fig. 3. Sorted partial Hausdorff distances $h_K(B,A)$ and their convergence to the optimal set $h_K(T^*(B),A)$ using $\lambda = 0.7$ for the simulation with NP=100% and NL=10.

where (r^s, θ^s) and the measurement range and bearing (sensor coordinates). The variables β_r, β_θ are assumed to be common to all points and account for sensor measurement errors induced by biases in range and bearing, respectively, while η_x and η_y are assumed to be zero-mean Gaussian noises arising from errors in the matching, as will be explained next. The range bias β_r results from errors in leveling the sensor (azimuth error). The bearing bias β_θ describes the rotation that suffers the measurement image due to misalignments of the sensor base with respect to the robot. Since normally ladar sensors are fixed and do not rotate with respect to the platform, it becomes difficult to determine β_θ without an additional heading sensor, such as a compass, because the main rotation of the measurement image results from the rotation θ of the robot as it moves and turns. Thus, it is assumed here that $\beta_\theta = 0$.

Employing (2), a *measurement image* can be created from the N measurement samples by setting all pixels to zero except for those at the coordinates z_i^w, $i = 1, ..., N$, which must be set to one. Similarly, the environment map, such as a CAD floor plan drawing must be rasterized, i.e. the drawing must be sampled discretely to create a *model image* in which pixels are set to one wherever there is a geometric element or to zero otherwise. The resolution of both (measurement and model) images should be sufficiently large, in order to allow for accurate position estimates, but should not exceed a value such that each pixel represents a dimension far smaller than the precision of the sensor itself.

Labeling the model image by A and the measurement image by B, the matching algorithm presented previously can be employed to estimate the values of x, y and θ, as well as η_r, through the solution of (1), which yields a transformation T^* that minimizes (8). The transformation T^* can be parametrized by a translation $\delta = (x, y)$, a rotation by θ, and scaling α, such that $\alpha\, r_i^s = r_i^s + E(\eta_r)$, where $E(\eta_r)$ denotes the expected value of η_r. Thus the solution of (8) that minimizes the difference between the model and measurement image naturally results in an observation of the robot's location and orientation. In practice, the matching process is not perfect because the sensor and the model have a finite resolution, and also the sensor measurements may be affected by clutter and occlusions, which limit the precision of the results. On the other hand, the actual transformation from polar to Cartesian coordinates in (2) also produces deformations of the objects in the image. Thus, to account for these sources of error, the noises η_x and η_y need to be included in the measurement model given in (2).

Despite these errors, the accuracy of the position and orientation estimates can be further improved using an extended Kalman filter (EKF), which additionally allows to obtain estimates of the robot's velocity and the sensor range bias β_r, as shown in the next section.

IV. EXPERIMENTAL RESULTS

The proposed localization approach was evaluated using an ActivMedia® Pioneer 3 All Terrain (P3-AT) differential drive robot carrying a Sick® PLS-101 Laser range finder, shown in Fig. 4. The sensor was set to scan $180°$ with a range span of 0 to 50 m. Its range accuracy is of the order of ± 0.05 m with a resolution of 0.07 m or better and an angular resolution of $0.5°$. The 360 samples covering the full distance range and angular sweep obtained with this system configuration have proven sufficient to ensure an accurate matching.

Fig. 4. P3-AT differential drive robot with a Sick PLS-101 ladar.

In order to implement the EKF, the following simplified model equation is employed to describe the motion of the robot:

$$\begin{bmatrix} \dot{x} \\ \dot{y} \\ \dot{\theta} \\ \dot{v}_R \\ \dot{v}_L \\ \dot{\beta}_r \end{bmatrix} = \begin{bmatrix} \frac{v_R+v_L}{2}\sin(\theta) + \xi_x \\ \frac{v_R+v_L}{2}\cos(\theta) + \xi_y \\ \frac{v_R-v_L}{L} + \xi_\theta \\ u_1 + \xi_{u_1} \\ u_2 + \xi_{u_2} \\ u_3 + \xi_{u_3} \end{bmatrix} \stackrel{def}{=} f(x,u) \quad (3)$$

where ξ_x, ξ_y, ξ_θ, ξ_{u_1}, ξ_{u_2} and ξ_{u_3} are all assumed to be zero-mean, i.i.d. Gaussian process noises. The above model corresponds to the standard kinematic model for a differential drive robot [1], augmented to include the accelerations $\dot{v}_R$ and $\dot{v}_L$ of the left and right wheels, which are controlled through the commands u_1 and u_2, respectively. It is to be noted that using the velocities of each wheel is equivalent to including terms for the longitudinal velocity v of the robot's mass center and its angular rate of change ω, since $v = (v_R + v_L)/2$ and $\omega = (v_R - v_L)/L$. Inertia moments and masses are not explicitly considered in the model because the EKF can automatically compensate and adjust the gain dynamically as needed. The model has also been augmented to include the unknown range bias, which is assumed to be constant throughout the experiment, and hence, the *virtual* input u_3 is set to zero.

Considering that the matching strategy automatically outputs the observations that feed the EKF, the following simple measurment model is employed:

$$\begin{bmatrix} z_1 \\ z_2 \\ z_3 \\ z_4 \end{bmatrix} = \begin{bmatrix} x + \zeta_x \\ y + \zeta_y \\ \theta + \zeta_\theta \\ \beta_r + \zeta_{\beta_r} \end{bmatrix} \stackrel{def}{=} h(x) \quad (4)$$

where ζ_x, ζ_y, ζ_θ and ζ_{δ_r} are assumed to be zero-mean i.i.d. Gaussian measurement noises.

To determine the performance of the proposed approach, a reference trajectory of known geometry was defined first. The experiment consisted in scanning the environment once every second while the robot followed the reference trajectory at a constant velocity of 5 cm/s. Thus the change in position between scans was about 5 cm. In order to find the transformation that minimizes the MHD, $\bar{h}_K(B, A)$ given in (8), the matching strategy described in the previous sections is applied with $\lambda = 0.7$, resulting in an almost perfect match as shown in Fig. 5. It is worth pointing out that the matching procedure is carried out successfully in spite of the large error in the initial state state and the presence of people walking around the robot as shown in the video.

The matching procedure is repeated after every ladar scan, yielding position, orientation and radar bias measurements that are fed to the EKF in order to obtain smoothed estimates of the robot's state vector. The estimated trajectory traversed in 100 seconds is shown in Fig. 6. The magnitude of the error between the estimated position and the actual trajectory coordinates is shown in Fig. 7, while the heading error is shown in Fig. 8. Both figures confirm that the estimation is reasonably good for most part of the trajectory except at the points in which the heading changes, such as at $t = 38$ seconds. The velocity estimates can be derived using the model equations (3). Thus, the forward velocity estimate is given by $\hat{v}(k|k) = (\hat{x}_4(k|k) + \hat{x}_5(k|k))/2$, while the turning velocity estimate is given $\hat{\omega}(k|k) = (\hat{x}_4(k|k) - \hat{x}_5(k|k))/L$, where L is the distance between wheels, and $\hat{x}_i(k|k)$, $i = 4, 5$ are the right and left wheel estimated velocities, respectively. Since the commands issued to the robot are constant throughout the piecewise linear trajectory, the estimates remain constant for most part of the trajectory, except at points where there are heading step changes. The turning ratio estimate is also constant and approximately zero, except at the turning point. Similarly, the estimated range bias remained constant throughout the experiment because the resolution of the rasterized model is equal to 5 cm per pixel and the resolution of the scanner is better than 7 cm, while its precision is within ± 5 cm.

The algorithm was implemented in Matlab® running on a 2.8 GHz Pentium IV computer with 512 MB RAM. Its execution period was verified to be on average below 0.10 s per scan consisting of 360 samples. The complexity of our algorithm is is smaller than $W \cdot O(N_s \log(N_s))$, where W is the largest axis of the reference map and N_s is the number of samples per scan. This complexity is similar to that of the best point-to-point or line-to-line localization approaches [9], e.g. Split-and-Merge with clustering.

V. Conclusions

A robust approach for estimating the position, heading and velocity of a mobile robot in a cluttered environment was presented. The approach relies on matching ladar measurements to a previously created map of the environment, such as an image of a rasterized floor plan drawing. Central to the matching process is the identification of a set of image transformations that minimize the modified Hausdorff distance (Appendix, eq. (8)). The advantages of incorporating this metric lies in the fact that (i) it can be applied to non-structured environments unlike most line-to-line matching techniques, (ii) it does not require to find one to one correspondences between points unlike traditional point-to-point methods, and (iii) it is more robust to outliers arising from clutter and occlusions than point-to-point or feature-to-feature methods. To further improve the position, heading and velocity estimates, the raw position and orientation measurements are passed to an EKF. The approach also allows to readily obtain the sensor's range bias as part of the matching process, and can be easily modified to obtain the sensor's bearing bias, if a heading sensor is added to the robot. The results obtained demonstrate the effectiveness of the approach as it yields rapidly converging accurate estimates

with a comparable computational cost to that of Split-and-Merge line extraction based localization algorithms, which are among the fastest.

Future work considers incorporating the MHD as part of the underlying matching process in Markov and Monte Carlo Localization schemes to assess the tradeoff between increased computational complexity and the possible improvement in the global localization capability. Continuing research also considers finding systematic approaches to dynamically adjusting the the number of samples that are rejected in the calculation of the MHD, as this may improve the accuracy of the measurements.

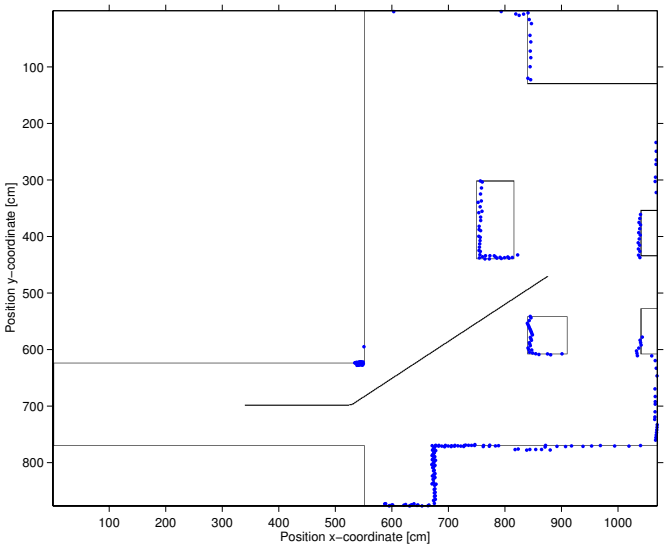

Fig. 5. Matching of the measurements (points) to the model (thin lines).

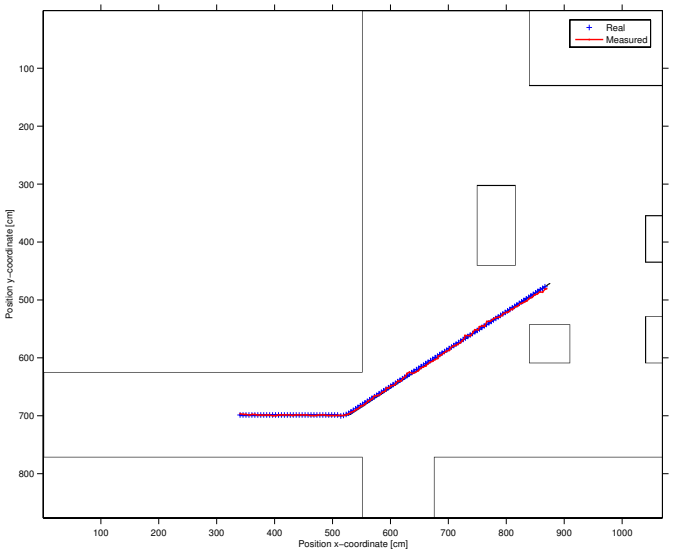

Fig. 6. Estimated trajectory (black) and reference trajectory(gray) starting from $(x_0, y_0, \theta_0) = (340.5cm, 698.7cm, 0°)$ at $t_0 = 0[s]$, and ending in $(x_f, y_f, \theta_f) = (866.7cm, 477.3cm, 32.8°)$ at $t_0 = 122[s]$, with constant forward speed $v \approx 5[cm/s]$.

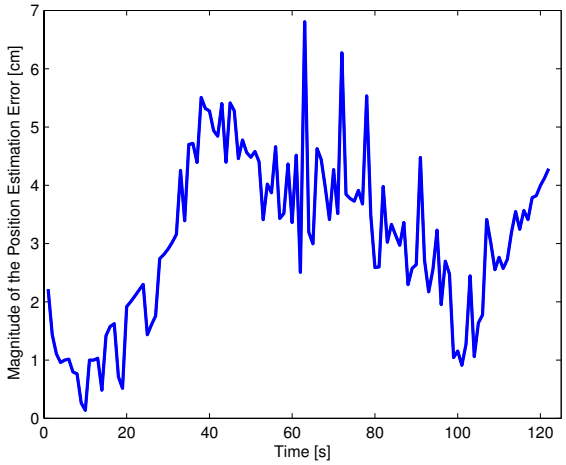

Fig. 7. Magnitude of the error between the estimated position and the real trajectory coordinates.

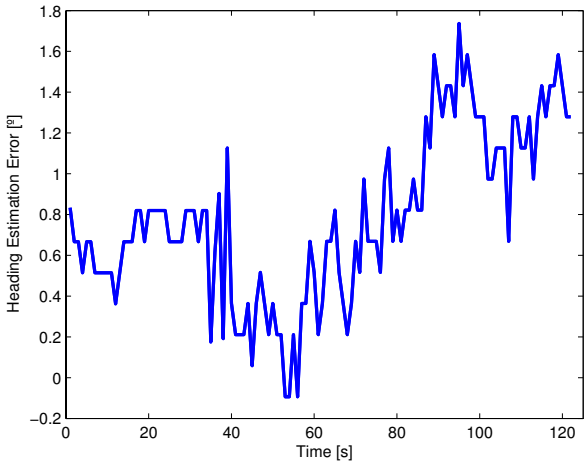

Fig. 8. Error between the estimated heading angle and the real trajectory direction.

ACKNOWLEDGMENTS

This project has been supported by the National Commission for Science and Technology Research of Chile (Conicyt) under Fondecyt Grant 11060251.

APPENDIX

MODIFIED HAUSDORFF DISTANCE

The computation of the Hausdorff distance is a technique to measure the degree of dissimilarity among different objects. By taking two sets of points, one being the reference model and the other the actual measurements, the HD between them is small when every point in one of the sets is near to some point in the other. Given two sets, $A = \{a_1, a_2, \ldots, a_p\}$ and $B = \{b_1, b_2, \ldots, b_q\}$, the HD between A and B is defined as:

$$H(A, B) \stackrel{def}{=} \max(h(A, B), h(B, A)) \quad (5)$$

where

$$h(A, B) \stackrel{def}{=} \max_{a \in A} \min_{b \in B} \|a - b\| \quad (6)$$

is the directed HD between sets A and B.

Numerical procedures to compute this distance, sort the points in A according to their distance to the nearest point in B and then select the farthest one as the result. For instance, if $h(A,B) = h^*$, then every point in A is at most at a distance h^* of a point in B. The point with distance h^* is the point that most deviates from set B. Figure 9 shows a geometric representation of the HD as applied to pattern recognition. Here sets A and B are the reference model and measurements, respectively. By rotating and translating the measurements, a satisfactory matching is obtained as the one that minimizes $H(A,B)$.

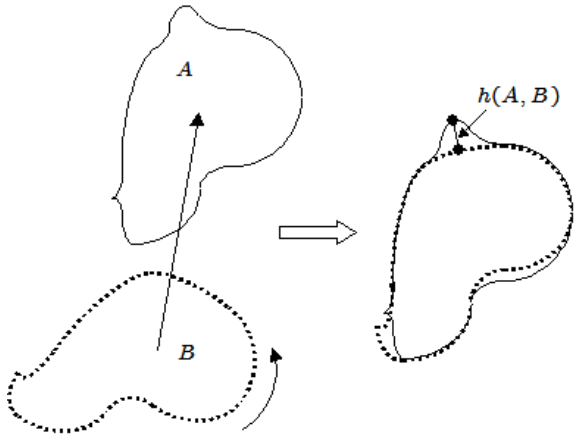

Fig. 9. Pattern matching employing the Hausdorff distance.

In order to reduce the number of calculations, a distance transform in the form of a Voronoi matrix is computed first. By doing so, set A is processed only once. Further details can be found in the paper by W. Rucklidge [12].

In most applications the sets A and B are not identical, as would typically occur in the presence of occlusions, measurement noise and image distortions. The latter is particularly valid for ladar images generated through the application of a transformation of the raw measurements in polar coordinates to a set of measurements in Cartesian coordinates, so offsets in range will cause a shrinkage or enlargement of the objects. Sometimes these differences can also be introduced at intermediate stages, such as expansion, rotation and translation, among other.

All these sources of error will generate some false-positive matches with Hausdorff distances significantly larger than the one of any true-positive match. Taking advantage of the fact that the HD computation procedure determines the distance of the farthest point in B by ranking the distances of its points to points in A, a way of reducing erroneous matches is to select the K^{th} distance in the ranking, instead of the largest one [12]. In other words, some of the the points in B with the largest distances are ignored and only a subset is used. The HD with respect to A of this subset of B is the so-called *partial (directed) HD*. In order to formally define the partial HD, it is convenient to introduce first a mapping d_Ω:

$$d_\Omega : x \rightarrow d_\Omega(x) = \min_{\omega \in \Omega} \|x - \omega\|$$

that *measures* the distance of the closest point ω in a set Ω to some point x. Then the partial HD of the K *best matching* points of the measurements set B to the model set A can be defined recursively for $K = q, q-1, q-2, \ldots, 2, 1$ as:

$$h_K(B,A) = \max_{b \in B^K} d_A(b) \qquad (7)$$

where $B^K = B^{K+1} - \{b^*_{K+1}\}$, $b^*_K = \arg\max_{b \in B^K} d_A(b)$ and the initial values $B^{q+1} = B$, $b^*_{q+1} = \{\emptyset\}$. It is worth noting that $h_q(B,A) = h(B,A)$, and that $h_q(B,A) \geq h_{q-1}(B,A) \geq \cdots \geq h_1(B,A)$, since $B^q \supset B^{q-1} \supset \cdots \supset B^1$. Hence, this definition automatically implies that there are K measurement points in B within a distance $h_K(B,A)$ from A (the K^{th} partial HD). Since more than one transformation of the image associated with the measurements set may result in similar values for $h_K(B,A)$, an effective criteria for successful matching is to minimize the average of partial Hausdorff distances smaller or equal to $h_K(B,A)$ for some chosen K. This average, also known as *modified* HD [12], is given by:

$$\bar{h}_K(B,A) = \frac{1}{K} \sum_{i=1}^{K} h_i(B,A) \qquad (8)$$

Employing the modified HD, ensures that more points in the image will resemble the model. For practical purposes, it is convenient to define the ratio of model points employed in the calculation of the average as $\lambda = K/q$. Then, K may be selected in terms of the ratio λ, simply as $K = \lambda\, q$, with $1/q \leq \lambda \leq 1$. The value of λ is found empirically as the one that minimizes the matching error for a set of image and model pairs.

REFERENCES

[1] S. Thrun, W. Burgard, and D. Fox, *Probabilistic Robotics*, MIT Press, 2005.

[2] S. Iyengar and A. Elfes, *Autonomous Mobile Robots*, IEEE Computer Society, 1991.

[3] J. D. Tardós, J. Neira, P. Newman, and J. Leonard, "Robust mapping and localization in indoor environments using sonar data," *Int. J. Robotics Research*, vol. 21, no. 4, pp. 311–330, 2002.

[4] O. Wulf, D. Lecking, and B. Wagner, "Robust self-localization in industrial environments based on 3D ceiling structures," *Proc. IEEE/RSJ Int. Conf. Intelligent Robots and Systems*, pp. 8–12, 2006.

[5] N. Karlsson, E. Di Bernardo, J. Ostrowski, L. Goncalves, P. Pirjanian and M. E. Munich, "The vSLAM algorithm for robust localization and mapping", *Proc. IEEE Int. Conf. Robotics and Automation*, pp. 24–29, 2005.

[6] A. Diosi and L. Kleeman, "Advanced sonar and laser range finder fusion for simultaneous localization and mapping," *Proc. IEEE/RSJ Int. Conf. Intelligent Robots and Systems*, pp. 1854–1859, 2004.

[7] G. A. Borges and M.-J. Aldon, "Line extraction in 2D range images for mobile robotics," *J. of Intelligent and Robotic Systems*, v. 40, pp. 267–297, 2004.

[8] L. Zhang and B. K. Ghosh, "Line segment based map building and localization using 2D laser rangefinder," *Proc. IEEE Int. Conf. Robotics and Automation*, pp. 2538–2543, 2000.

[9] V. Nguyen, A. Martinelli, N. Tomatis, and R. Siegwart, "A comparison of line extraction algorithms using 2D laser rangefinder for indoor mobile robotics," *Proc. IEEE/RSJ Int. Conf. Intelligent Robots and Systems*, pp. 1929–1934, 2005.

[10] J. Minguez, F. Lamiraux, and L. Montesano, "Metric-based scan matching algorithms for mobile robot displacement estimation," *Proc. IEEE Int. Conf. Robotics and Automation*, pp. 3557–3563, 2005.

[11] A. Diosi and L. Kleeman, "Laser scan matching in polar coordinates with application to SLAM," *Proc. IEEE/RSJ Int. Conf. Intelligent Robots and Systems*, pp. 3317–3322, 2005.

[12] W.J. Rucklidge, "Efficient visual recognition using the Hausdorff distance," *Int. J. Computer Vision*, vol. 24, pp. 251–270, 1997.

[13] A. Guesalaga, "Recursive estimation of radar biases using electronic charts," *IEEE Trans. Aerospace and Electronic Systems*, vol. 40, no. 2, pp. 725–733, 2004.

[14] D. P. Huttenlocher, G. A. Klanderman, and W. J. Rucklidge, "Comparing images using the Hausdorff distance," *IEEE Trans. Pattern Analysis and Machine Intelligence*, vol. 15, no. 9, pp. 850–863, 1993.